The EMBO Journal vol.13 no.15 pp.3638–3647, 1994

Three ARS elements contribute to the *ura4* replication origin region in the fission yeast, *Schizosaccharomyces pombe*

Dharani D.Dubey, Jiguang Zhu, Deborah L.Carlson, Karuna Sharma and Joel A.Huberman

Department of Molecular and Cellular Biology, Roswell Park Cancer Institute, Buffalo, NY 14263, USA

Communicated by H.Cedar

The *ura4* replication origin region, which is located near the *ura4* gene on chromosome III of the fission yeast, *Schizosaccharomyces pombe*, contains multiple initiation sites. We have used 2D gel electrophoretic replicon mapping methods to study the distribution of these initiation sites, and have found that they are concentrated near three ARS elements (stretches of DNA which permit autonomous plasmid replication). To determine the roles of these ARS elements in the function of the *ura4* origin region, we deleted either one or two of them from the chromosome and then assessed the consequences of the deletions by 2D gel electrophoresis. The results suggest that each of the three ARS elements is responsible for the initiation events in its vicinity and that the ARS elements interfere with each other in a hierarchical fashion. It is possible that the large initiation zones of animal cells are similarly composed of multiple mutually interfering origins.

Key words: ARS/origin/replication/replicator/*Schizosaccharomyces pombe*

Introduction

In eukaryotic organisms DNA replication begins at origins which are scattered irregularly along chromosomal DNA molecules. The 'replicators' (*cis*-acting sequences essential for origin function) responsible for origins have been defined in the budding yeast, *Saccharomyces cerevisiae*, where they correspond to ARS (autonomously replicating sequence) elements (Deshpande and Newlon, 1992; Rivier and Rine, 1992; Huang and Kowalski, 1993)—DNA fragments which permit plasmids to replicate autonomously in yeast cells and thus to transform yeast cells at high frequency (Hsiao and Carbon, 1979; Struhl *et al.*, 1979). Initiation sites, the positions in DNA molecules where the synthesis of new DNA strands begins, are determined by replicators. In the case of *S.cerevisiae* origins, results obtained with 2D gel electrophoretic mapping techniques (Brewer and Fangman, 1987; Huberman *et al.*, 1987) show that, within the resolution of the techniques (to within several hundred base-pairs), initiation sites colocalize with replicators (ARS elements; reviewed in Campbell and Newlon, 1991).

Available data do not permit such a clear understanding of replication origins in animal cells. Replicators are known to exist for three animal cell origins: the origin used to amplify the third chromosome chorion genes during *Drosophila* development (reviewed in Orr-Weaver, 1991), the origin located downstream of the dihydrofolate reductase gene in CHO cells (Handeli *et al.*, 1989) and the origin responsible for replicating the human β-globin gene domain (Kitsberg *et al.*, 1993). The replicators associated with the two mammalian origins are not well defined. The *Drosophila* replicator consists of several short (a few hundred base-pairs), partially redundant sequences (Orr-Weaver, 1991). Results obtained with a variety of techniques suggest that initiation sites at animal cell origins are distributed through regions, called initiation zones, of several kilobase-pairs or larger (reviewed in Burhans and Huberman, 1994). Within the initiation zones studied so far, initiation sites cannot be resolved by 2D gel electrophoresis. Progress in understanding the origins of animal cells has been hindered by lack of a reliable ARS assay and the difficulty of direct genetic manipulations in chromosomes.

For these reasons, we sought a genetically tractable model organism for study of origins associated with initiation zones. It seemed to us that the fission yeast, *Schizosaccharomyces pombe*, might serve this purpose. A reliable ARS assay is available for *S.pombe* (Maundrell *et al.*, 1988) and, like *S.cerevisiae*, *S.pombe* offers the advantages of small genome size and ease of genetic manipulation. Nevertheless, *S.pombe* is evolutionarily distant from *S.cerevisiae*, and in some respects it is more similar to animal cells. To determine whether initiation zones exist in *S.pombe*, we employed 2D gel methods to identify and preliminarily characterize a replication origin region near the *ura4* gene on chromosome III (Zhu *et al.*, 1992a). Results from this initial study suggested that the initiation sites of the *ura4* origin region were distributed through a zone of >4 kbp and could not be resolved from each other (Zhu *et al.*, 1992a). In this respect the *ura4* origin region appeared to resemble the origins of animal cells.

Here we report the combined results of higher resolution 2D gel electrophoresis and genetic studies of the *ura4* origin region. These results lead to the conclusion that what initially appeared to be a continuous initiation zone is actually a cluster of three closely spaced origins. Three ARS elements are essential components of the replicators of these origins. The three origins function in a hierarchy like a pecking order. All three origins interfere with each other, but the extent of interference differs between origins.

Results

Identification of ARS elements

As will be demonstrated in subsequent sections of this paper, initiation events in the *ura4* origin region can be

detected by 2D gel electrophoresis in the areas under the gray bars in Figure 1. An initial survey of restriction fragments covering and flanking these initiation sites revealed that both the 1.25 kbp *Eco*RI−*Bam*HI fragment and the 2.7 kbp *Bam*HI−*Eco*RI fragment (which together constitute the 4.0 kbp *Eco*RI fragment marked by a brace in Figure 1) contained ARS activity. To better localize ARS activity within these fragments, we employed progressive exonuclease III deletion from both ends of each fragment. The results of assays for ARS activity in selected members of each set of deletions are shown in Figure 2. It is evident that, within each of the two restriction fragments, a single region is essential for ARS activity. This region corresponds roughly to nucleotides 600–1200 in Figure 2A and nucleotides 3300–3800 in Figure 2B.

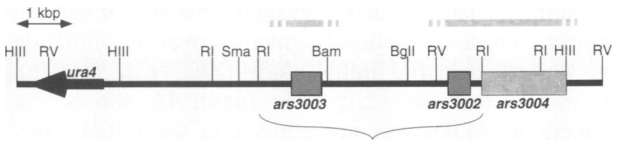

Fig. 1. The stretch of *S.pombe* chromosome III containing the *ura4* gene and replication origin region. The *ura4* gene is shown as a black arrow pointing in the direction of transcription. The two major, well characterized ARS elements are shown as gray boxes, and the third ARS element (*ars3004*) is shown as a lighter, longer gray box, because it is weaker and because it has not yet been better localized. The regions containing initiation sites detectable by 2D gel electrophoresis are indicated by gray bars above. The nucleotide sequence of the *Eco*RI fragment indicated by the brace has been determined (J.Zhu, D.Carlson, D.Dubey, K.Sharma and J.A.Huberman, submitted) and is available in the EMBL Data Library (accession number Z27236) and in GenBank (accession number L25861). Bam, *Bam*HI; BgII, *Bgl*II; HIII, *Hin*dIII; R, *Eco*RI; RV, *Eco*RV; Sma, *Sma*I.

During the course of these experiments, a third ARS element with ~4-fold lower transformation frequency than the other two ARS elements was identified in the *Eco*RI−*Hin*dIII fragment to the right of the other two ARS elements (Figure 1). This third ARS element has not yet been better localized.

ARS elements in *S.pombe* have previously been assigned names in arbitrary fashion. A systematic ARS-naming convention similar to that proposed for *S.cerevisiae* by Campbell and Newlon (1991) would be beneficial. We suggest that ARS elements in *S.pombe* be assigned 4-digit names. The first digit would indicate the chromosome on which the ARS element is located, and the next three digits would be a unique identifier for each ARS element. ARS elements would ordinarily be named in the order of their discovery. Because an ARS element has already been discovered on chromosome III (an ARS element in each copy of the ribosomal DNA repeat; Toda *et al.*, 1984), we have assigned the names *ars3002*, *ars3003* and *ars3004* to the three new ARS elements described here (Figure 1).

Characterization of the ura4 origin region in D18 cells

To identify the roles of these ARS elements in the establishment, strength and location of the *ura4* origin region, we planned to delete *ars3002* and *ars3003* from

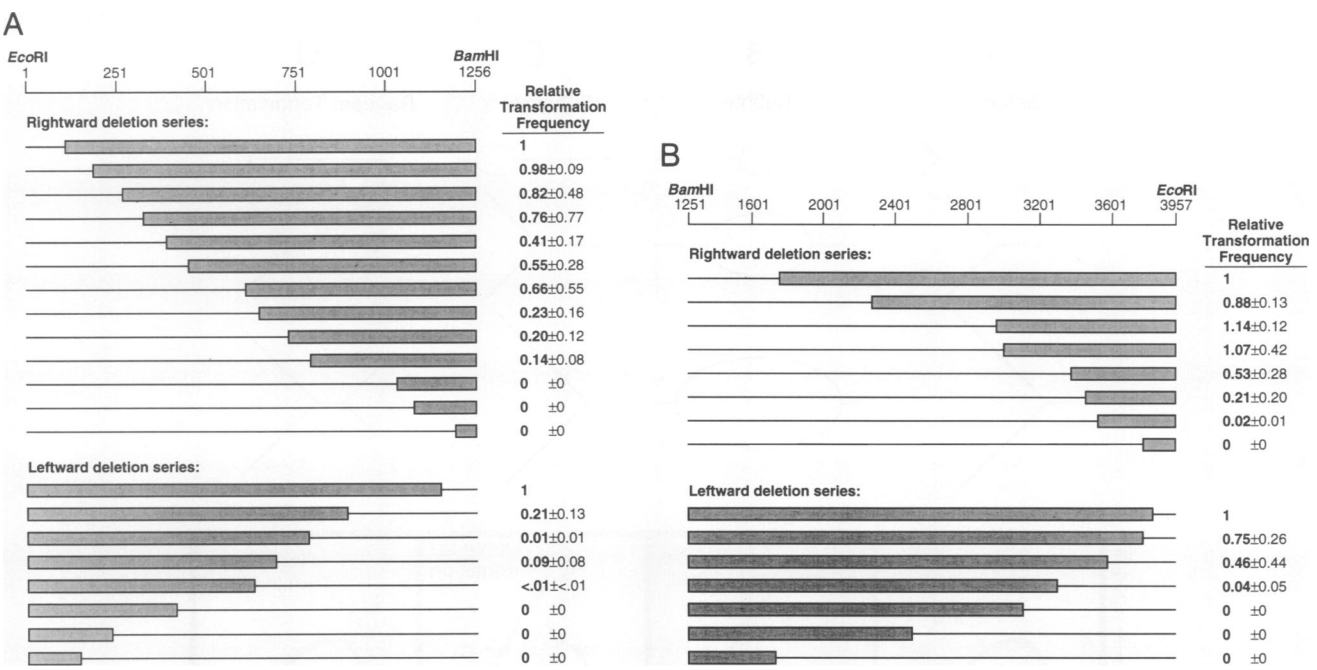

Fig. 2. Localization of the two major ARS elements of the *ura4* replication origin region. The two adjacent restriction fragments analyzed in this figure correspond (**A**) to the 1.25 kbp *Eco*RI−*Bam*HI fragment and (**B**) to the 2.7 kbp *Bam*HI−*Eco*RI fragment in the braced region of Figure 1. The scales at the tops of (A) and (B) show nucleotide positions as defined in the nucleotide sequence of the braced region (see Figure 1 legend). Notice the difference in scale between (A) and (B). The gray bars represent the *S.pombe* DNA contained in each analyzed plasmid. The thin lines represent the portions of *S.pombe* DNA which were removed by deletion and replaced by vector sequences. To compensate for variations in transformation efficiency between experiments, the values for each series were normalized to the transformation frequency obtained with the shortest deletion in that series. For each deletion, the normalized values from three or four independent experiments were averaged. The average values, with their standard deviations, are shown. The ranges of the transformation frequencies obtained for the shortest deletion in each series are: (A) rightward deletions, 4800–52 200 colonies/μg; (A) leftward deletions, 4700–8900 colonies/μg; (B) rightward deletions 34 000–70 000 colonies/μg; (B) leftward deletions 34 000–68 000 colonies/μg.

the chromosome and then use 2D gel electrophoretic techniques to characterize replication of the altered region.

For construction of genomic alterations, we chose to use the *ura4-D18* strain, hereafter referred to as D18, in which the 1.8 kbp *Hin*dIII fragment containing the *ura4* gene has been deleted (Grimm *et al.*, 1988), thus permitting selection for new inserts containing the *ura4* gene. Because the strain in which the *ura4* origin region was originally characterized (strain 975h^+; Zhu *et al.*, 1992a) contained the *ura4* gene in its normal location just a few kbp away from the origin region (Figure 1), we thought it possible that the *ura4* gene deletion in the D18 strain might have affected *ura4* origin region function. For this reason, we considered it necessary, before using the D18 strain to construct genomic deletions, to characterize origin function in the D18 strain and determine whether it was different from that in the 975h^+ strain.

For this purpose, we employed the neutral/neutral 2D gel technique of Brewer and Fangman (1987). This technique separates replication intermediates according to their shapes, as shown in Figure 3. Restriction fragments passively replicated by an external origin generate Y arcs (Figure 3A), while fragments containing an internal origin form bubble-shaped intermediates, which generate a high-rising bubble arc after 2D gel electrophoresis (Figure 3B). An asymmetrically located origin generates the early portion of a bubble arc and the late portion of a Y arc (Figure 3C). Note, however, that the internal origin must be within the central third of the restriction fragment to be assured of producing a detectable bubble arc (Linskens and Huberman, 1990). Fragments passively replicated by forks converging from two flanking origins generate termination signals. If termination can occur at any position within a restriction fragment, then a triangular signal like that in Figure 3D is produced. In the case of a mixed pattern, the relative intensity of each signal is indicative of the proportion of that type of replication intermediate in the total population.

The restriction fragments studied and the resulting autoradiograms are shown in Figure 4A. Fragments **a** and **h** (Figure 4A) and fragments to the left of **a** and to the right of **h** (unpublished data) do not produce detectable bubble arcs. However, fragments **b** and **g**, and most of the fragments between them, reveal bubble arcs of varying strengths. These restriction fragments cover the initiation zone described in our initial study (Zhu *et al.*, 1992a). The more extensive analysis in Figure 4A shows that fragment **d**, which was not utilized in the initial study (Zhu *et al.*, 1992a), does not generate a visible bubble arc. There are no detectable initiation events within its central third. Thus, the initiation zone appears to consist of one initiation region defined by the central thirds of fragments **b** and **c** and a second initiation region defined by the central thirds of fragments **e**–**g**. All of these fragments contain ARS elements within their central thirds. The strongest bubble arc is generated by fragment **e**, centered on *ars3002*, indicating that most initiation events are concentrated near *ars3002*.

In addition to bubble arcs, all fragments in Figure 4A also generate strong Y arcs, implying that each of them

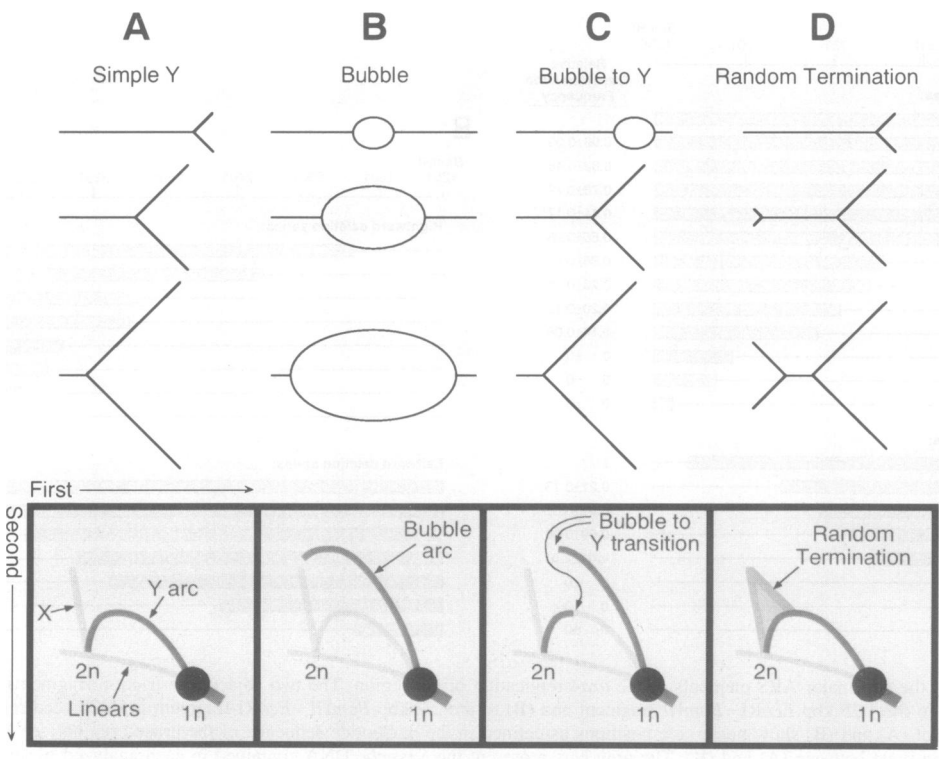

Fig. 3. Signals produced by various types of replicating restriction fragments subjected to neutral/neutral 2D gel electrophoresis (Brewer and Fangman, 1987). The arc of linears, X line (due to X-shaped recombination intermediates) and Y arc are shown in light gray in each example for reference purposes only; they do not always appear in actual experiments. The pattern expected for random termination was deduced by Zhu *et al.* (1992b), based on the assumption that converging replication forks might meet with equal probability at any position throughout the restriction fragment being studied.

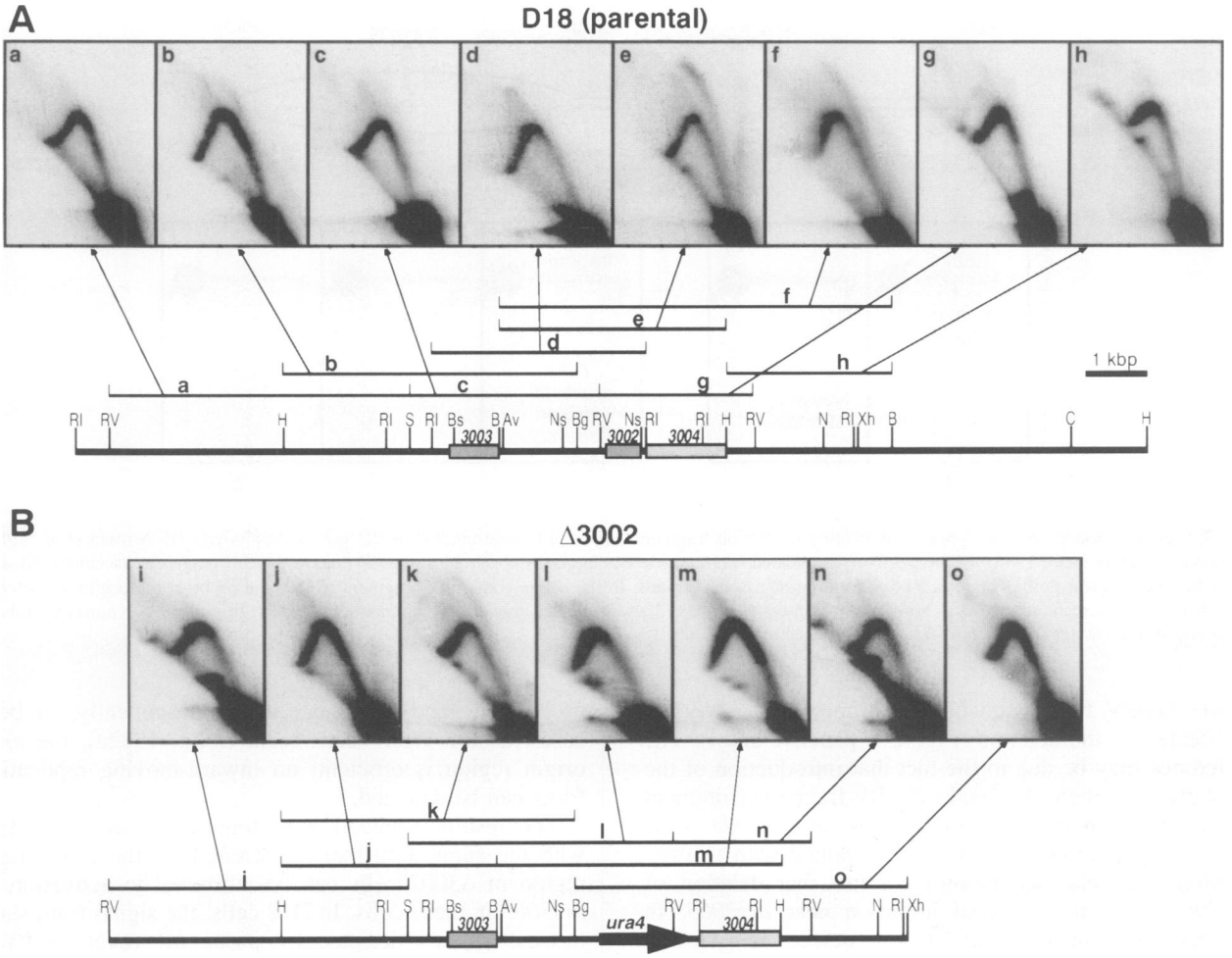

Fig. 4. Effects of deleting *ars3002* on the *ura4* origin region, as studied by neutral/neutral 2D gel electrophoresis. The restriction sites are: RI, *Eco*RI; RV, *Eco*RV; H, *Hin*dIII; S, *Sma*I; Bs, *Bst*BI; B, *Bam*HI; Av, *Avr*II; Ns, *Nsi*I; Bg, *Bgl*II; N, *Nru*I; C, *Cla*I. (**A**) The initiation zone associated with the *ura4* origin region can be resolved into two separate initiation regions, each associated with one or two ARS elements. (**B**) Deletion of *ars3002* drastically reduces the initiation frequency in fragment **m** and enhances it in fragment **k**.

is frequently replicated passively or by an origin located near its end. In each case, a faint triangular random termination signal is also visible, suggesting that termination (merging of converging replication forks) occurs throughout the ARS-containing region (Zhu *et al.*, 1992b). The putative termination signal is stronger for fragment **d** and weaker for fragments **a** and **h**, and fragments beyond **a** and **h** generate Y arcs with either fainter or no detectable triangular signals (unpublished data).

All these features are consistent with those previously detected for the *ura4* origin region in strain $975h^+$ (Zhu *et al.*, 1992a). However, the more detailed study in Figure 4A reveals that what was previously interpreted as a continuous initiation zone can in fact be resolved into two smaller initiation regions, one located over *ars3003* and the other located over *ars3002* and *ars3004*. As we describe below, neutral/alkaline 2D gel analysis of the *ura4* origin region in the D18 strain shows that, as in $975h^+$, replication forks move only outward from this origin region. Thus, neither the location, size nor the strength of the *ura4* origin region is detectably different between the D18 and $975h^+$ strains. We concluded that the D18 strain could be used for genetic studies of *ura4* origin region function.

Effects of deleting ars3002

The strongest initiation activity at the *ura4* origin region is near *ars3002* (Figure 4A, panel e). We reasoned that, if this ARS is responsible for the initiation activity in its vicinity, then its deletion should cause either loss or redistribution of initiation activity. To test this possibility, we substituted the chromosomal *ars3002* with the 1.8 kbp *Hin*dIII fragment containing the *ura4* gene (Figure 4B). This fragment has no ARS activity in a plasmid and no effect on *ura4* origin region activity when inserted into chromosome III next to *ars3002* in either orientation (unpublished data). After deletion of *ars3002*, the *Bam*HI–*Hin*dIII fragment which previously produced the strongest bubble arc (Figure 4A, panel e) now yields either no or just a barely detectable bubble arc, but it produces a stronger termination signal (Figure 4, panel m). Clearly, *ars3002* is essential for the major initiation activity in this region.

After removal of *ars3002*, the *Hin*dIII–*Bgl*II fragment containing *ars3003* generates a somewhat stronger, more complete bubble arc (Figure 4, panels b and k), suggesting that deletion of *ars3002* may increase the activity of *ars3003*. However, the bubble arc signal from the

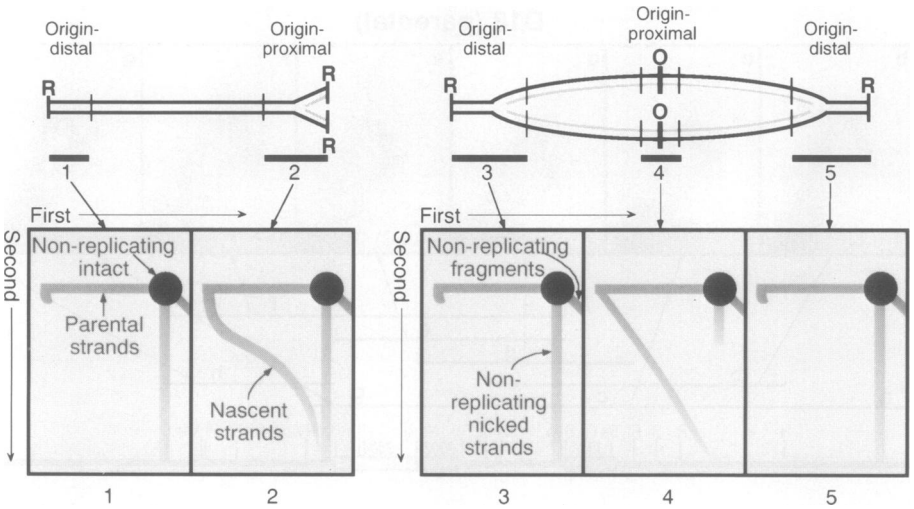

Fig. 5. Signals produced by two types of replicating restriction fragment subjected to neutral/alkaline 2D gel electrophoresis (Huberman *et al.*, 1987; Nawotka and Huberman, 1988). In the passively replicated fragment (left), the origin-proximal probe (2) detects the full range of nascent strand sizes while the origin-distal probe (1) detects only the longest nascent strands. In the origin-containing fragment (right), the probe at the origin (4) detects the full range of nascent strand sizes, while the origin-distal probes (3 and 5) detect only the longest nascent strands. In general, the closer a probe is to an origin, the shorter the nascent strands it can detect.

*Sma*I−*Eco*RV fragment which also contains *ars3003* is unaffected by the deletion (Figure 4, panels c and l). The difference may be due to the fact that introduction of the *ura4* gene lengthens the *Sma*I−*Eco*RV fragment (fragment **l** is longer than fragment **c**), so most of *ars3003* is no longer in its central third. Results obtained with neutral/alkaline 2D gels (see below) confirm that deletion of *ars3002* leads to increased initiation near *ars3003*. In contrast, deletion of *ars3002* has no detectable effect on the magnitudes of bubble arcs generated by restriction fragments containing *ars3004* (Figure 4, panels g, n and o).

The *ura4* origin region is efficient in both wild-type and D18 cells; no replication forks can be detected moving into it (Zhu *et al.*, 1992a; this paper). To determine whether the origin region remains efficient, even after deletion of *ars3002*, we employed neutral/alkaline 2D gel electrophoresis, which provides information about direction of replication fork movement (Huberman *et al.*, 1987; Nawotka and Huberman, 1988). First dimension electrophoresis separates restriction fragments according to extent of replication (Figure 5). The alkaline second dimension electrophoresis denatures DNA so that nascent strands are separated from parental strands and fractionated according to their sizes. Blots of the gels are then hybridized with probes from different parts of the fragment of interest. The closer the probe to the origin, the smaller the detected nascent strands, as shown in Figure 5 for a passively replicated and an origin-containing fragment.

We found the analysis of directions of replication within the three large *Eco*RI fragments which span the *ura4* origin region and flanking regions to be especially informative (Figure 6). Each of these fragments (named *a*, *b* and *c*, from left to right) were probed with left- and right-end probes (named *a*L, *a*R, etc.). The results obtained for D18 cells for fragments *a* and *c* (unpublished data) were similar to those shown for Δ3002 cells (Figure 6B). In both cases, the outer probes (*a*L and *c*R) failed to detect signals from short or intermediate-sized nascent strands, but the inner probes (*a*R and *c*L) succeeded. Consequently, in both cases, as for 975h^+ cells (Zhu *et al.*, 1992a), the *ura4* origin region is efficient; no inward-moving replication forks can be detected.

The results obtained with fragment *b* are consistent with the suggestion that the strength of the *ura4* origin region in Δ3002 cells can be attributed to activation of *ars3003* in these cells. In D18 cells, the signal from short nascent strands detected by probe *b*R (over *ars3002*) appears somewhat stronger than the signal detected by probe *b*L (over *ars3003*), suggesting that, in this fragment, replication forks move mostly from right to left (Figure 6A). In contrast, in Δ3002 cells, the signal from short nascent strands detected by probe *b*L is significantly stronger than that detected by *b*R (Figure 6B), indicating that, in this fragment, replication forks now move primarily from left to right.

These results were further confirmed by neutral/alkaline 2D gel analysis of the 7.7 kbp *Hin*dIII fragment containing the *ura4* origin region (Figure 7). This fragment had previously been studied in 975h^+ cells and had been found to yield only barely perceptible signals from the shortest nascent strands, even though it contains an efficient origin region (Zhu *et al.*, 1992a). Similarly, in the case of D18 cells, all probes within this fragment yielded little or no signal for short nascent strands (Figure 7A, probes αL and αM, and unpublished data). Therefore, to confirm that there was no selective loss of short nascent strands in this DNA preparation, the *Hin*dIII membrane from D18 cells was hybridized with probes βL and βR, which detect the origin-proximal and origin-distal ends, respectively, of the adjacent 7.4 kbp *Hin*dIII fragment. Probe βL detected nascent strands of all sizes, while probe βR failed to detect short nascent strands (Figure 7A). Therefore, the D18 DNA preparation contained short nascent strands, and the 7.4 kbp *Hin*dIII fragment is replicated from left to right. In Δ3002 cells, in contrast to D18 cells, probe αM, which is located over *ars3003*, detected significant

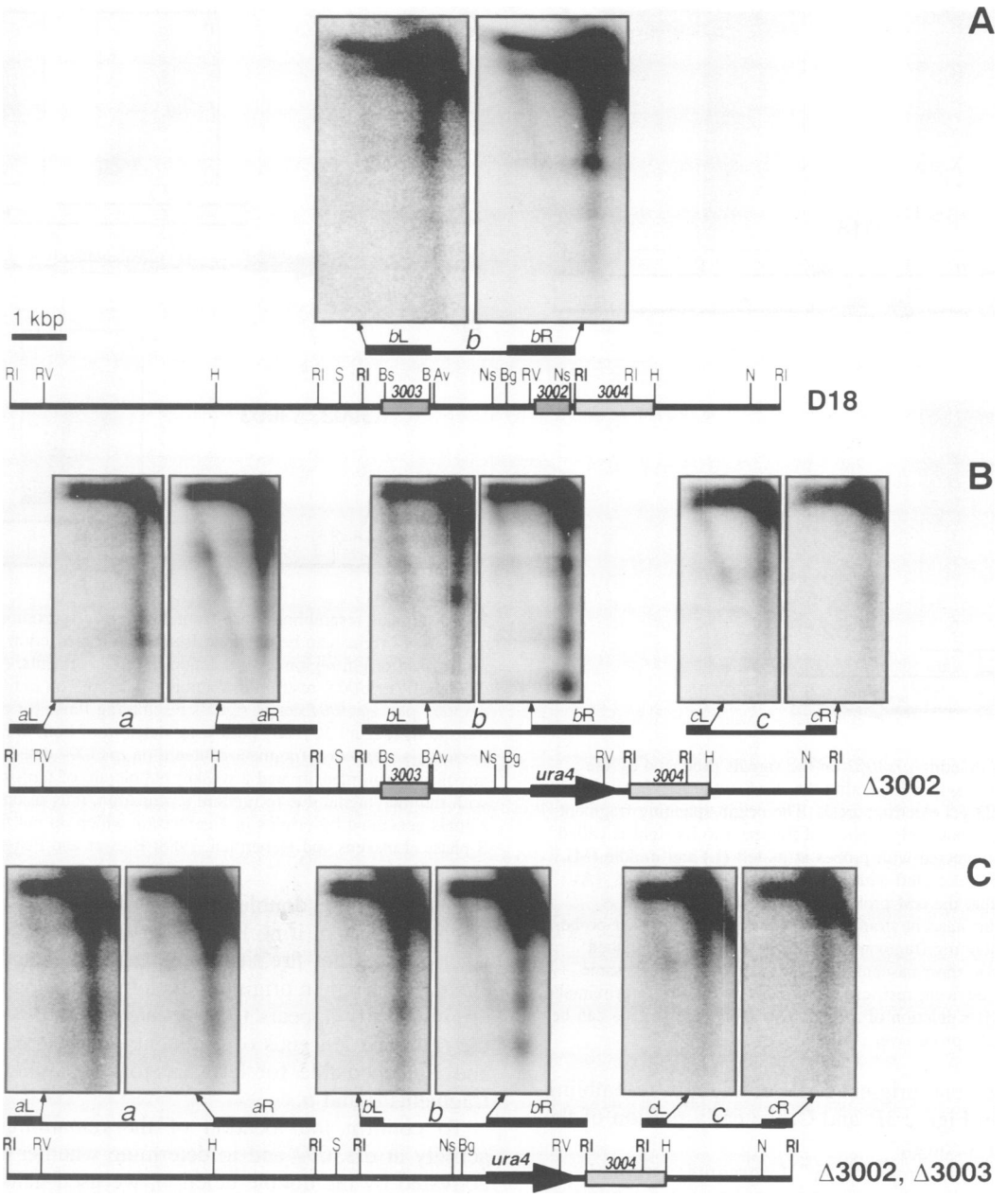

Fig. 6. Effects of deleting *ars3002* and *ars3003* on the signals produced by *Eco*RI restriction fragments spanning the *ura4* origin region, after neutral/alkaline 2D gel electrophoresis. The three *Eco*RI fragments of interest, called *a*, *b* and *c*, were detected by short probes from their left (L) or right (R) ends. (**A**) In the parental strain, D18, most replication forks in fragment *b* move from right to left; some move in the opposite direction. (**B**) After deletion of *ars3002*, most replication forks in fragment *b* now move from left to right; some move in the opposite direction. However, in fragments *a* and *c*, replication forks appear to move only outwards; none can be detected entering at the left end of fragment *a* or at the right end of fragment *c*. (**C**) After deletion of both *ars3002* and *ars3003*, replication forks move in both directions with approximately equal frequency through fragments *a* and *b*. They continue to move only rightward through fragment *c*.

signal from short nascent strands (Figure 7B), consistent with activation of *ars3003* by deletion of *ars3002*.

Effects of deleting ars3003

Deletion of *ars3003* does not diminish the strength of the *ura4* origin region (Figure 8A, and unpublished neutral/alkaline data). Instead, it leads to increased initiation activity in the vicinity of *ars3002* and *ars3004*. The bubble arcs from the *Bam*HI−*Hin*dIII fragment centered on *ars3002* and from the larger *Bam*HI fragment centered on *ars3004* become somewhat stronger (compare Figure 4, panels e and f with Figure 8A, panels a and b). In Δ3003 cells (Figure 8A, panels a and b), the early portion of the Y arc is weakened, so that a clear bubble to Y transition (as in Figure 3C) becomes visible. Similar changes occur at *ars3003* in Δ3002 cells (compare Figure 4, panels b and k). These alterations suggest that, after deletion of one of the two efficient ARS elements from the *ura4* origin region, initiation activity is enhanced near the other element, permitting the generation of 2D gel signals which more closely resemble those produced by origins in *S.cerevisiae* (note: in *S.cerevisiae*, restriction fragments

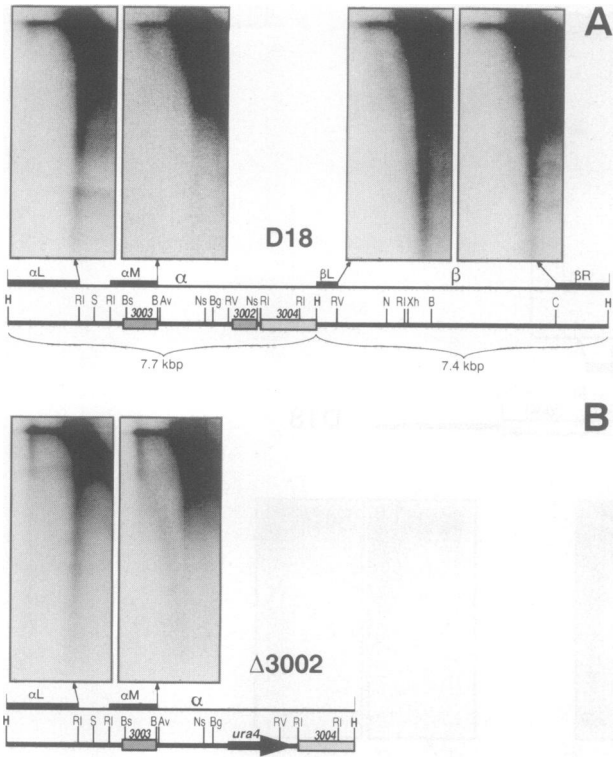

Fig. 7. Effects of deleting *ars3002* on the signals produced by the *Hin*dIII restriction fragment spanning the *ura4* origin region, after neutral/alkaline 2D gel electrophoresis. The origin-spanning fragment is called α, and the passively replicated fragment to its right is called β. Fragment α is detected with probes at its left (L) and middle (M), while fragment β is detected with left (L) and right (R) probes. (**A**) Despite the fact that the αM probe is over *ars3003*, no signal is detected from short nascent strands. The same is true for other probes in this origin-containing fragment (Zhu *et al.*, 1992a; unpublished data). Nevertheless, short nascent strands are detected on the same membrane in the adjacent restriction fragment by the origin-proximal probe, βL. (**B**) After deletion of *ars3002*, short nascent strands can be detected by the αM probe over *ars3003*.

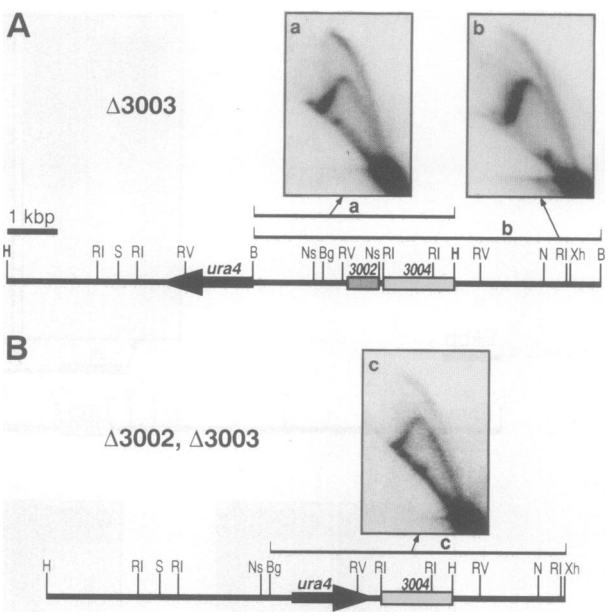

Fig. 8. Signals resembling those from *S.cerevisiae* chromosomal replication origins can be obtained from certain restriction fragments in the *ura4* origin region after deletion of ARS elements. (**A**) After deletion of *ars3003*, restriction fragments centered on *ars3002* or *ars3002* plus *ars3004* detect signals resembling those for bubble to Y transitions (Figure 3C). (**B**) Following deletion of both *ars3002* and *ars3004*, a restriction fragment centered on *ars3004* detects a strong Y arc of uniform intensity and a weaker bubble arc of uniform intensity, with minimal signal due to random termination, thus resembling the signals generated by origins in *S.cerevisiae* which do not fire in every S phase (Linskens and Huberman, 1988; Brewer and Fangman, 1993).

containing efficient origins generate signals resembling those shown in Figure 3B and C; the early portion of the Y arc is never strong).

Although both restriction fragments studied in Figure 8A contain portions of *ars3002* and *ars3004* in their central thirds, it is likely that their strong bubble arcs are primarily a consequence of activation of *ars3002*. When both *ars3002* and *ars3003* are deleted (Δ3002, Δ3003), the bubble signal due to initiations at *ars3004* alone is relatively weak (Figure 8B) and could not account for the strong bubble arc seen in Figure 8A.

Effects of deleting ars3002 and ars3003 together

To assess the effects of simultaneously deleting both efficient ARS elements (*ars3002* and *ars3003*), we used neutral/alkaline 2D gel electrophoresis to analyze the replication patterns of the relevant *Eco*RI fragments in the strain Δ3002, Δ3003 (Figure 6C). Probes from both ends of fragments *a* and *b* detected nascent strands of all sizes, suggesting that forks enter these fragments from both directions. Fragment *c*, however, is replicated only from left to right, because probe *c*L detects a range of nascent strand sizes while probe *c*R detects no short or intermediate-sized nascent strands. These observations suggest that the double deletion so weakens the *ura4* origin region that it no longer fires in every S phase, and when it does not fire, it is passively replicated by forks emanating from an origin on the left. The remaining weak origin activity appears to be located at *ars3004* between the right and left ends of fragments *b* and *c*, respectively, and is responsible for leftward fork movement through fragments *a* and *b*.

To confirm the location of the remaining initiation activity at *ars3004* and to determine whether *ars3004* is activated by the double deletion, we used neutral/neutral 2D gel electrophoresis to study the replication of a restriction fragment centered on *ars3004*. The bubble arc signal from this fragment in Δ3002, Δ3003 cells (Figure 8B) is considerably stronger than the bubble arc signal from the same fragment in Δ3002 cells (Figure 4, panel o) or from the *Eco*RV fragment centered on *ars3004* in D18 cells (Figure 4, panel g), implying that the activity of *ars3004* is increased in Δ3002, Δ3003 cells. However, this activation does not fully compensate for the loss of *ars3002* and *ars3003*; in Δ3002, Δ3003 cells the region is partly [~50%, based on visual comparison of nascent strand signals (Figure 6C, fragment *a*)] replicated by an external origin located somewhere to the left.

Discussion

The ura4 origin region contains three closely spaced origins

Initial characterization of the *ura4* origin region suggested that it consisted of a single initiation zone of ~4 kbp within

which discrete initiation sites could not be distinguished by 2D gel electrophoretic methods (Zhu *et al.*, 1992a). The results presented in this paper reveal that this initial impression was incorrect. The initiation zone can be resolved into two separate initiation regions. The left-hand region colocalizes with *ars3003*. The right-hand region extends over both *ars3002* and *ars3004*.

Colocalization of the initiation sites of the *ura4* origin region with three ARS elements suggests that these ARS elements may comprise or be essential components of replicators (*cis*-acting sequences essential for origin function). To test this possibility, we deleted *ars3002* and/or *ars3003* from the chromosome and then used 2D gel analyses to test the consequences of the deletions for chromosomal origin activity. We found that, when either *ars3002* or *ars3003* is deleted, initiation events are either dramatically reduced or completely removed from the immediate vicinity of the deletion (Figures 4, panels e and m, and 6A and B). Thus, *ars3002* and *ars3003* correspond to or are essential components of replicators of the *ura4* origin region. This observation complements the recent demonstration by Caddle and Calos (1994) that a plasmid replication origin colocalizes with an ARS element in *S.pombe*.

After deletion of *ars3002* and/or *ars3003*, initiation activity becomes more intense at the stronger of the remaining ARS elements (Figures 4B, 6B and C, 7B and 8), and the resulting 2D gel patterns more closely resemble those produced by *S.cerevisiae* origins, either efficient (Figures 6B, 7B and 8A) or inefficient (Figures 6C and 8B). Thus, what was originally defined as the *ura4* origin (Zhu *et al.*, 1992a) appears to consist of three closely spaced origins, each determined by a single ARS element as in *S.cerevisiae*. It would seem more appropriate to call this a 'compound origin' or an 'origin region'.

Interactions between closely spaced origins

There appears to be a hierarchical relationship like a pecking order between the three origins in the *ura4* origin region. In wild-type cells, the *ars3002*-associated origin is strongest; most initiation events occur in its vicinity (Zhu *et al.*, 1992a; Figure 4, panel e). When *ars3002* is deleted, the *ars3003*-associated origin is strengthened [Figures 4 (panel k), 6B and 7B], but the *ars3004*-associated origin remains relatively weak (Figure 4, panels n and o). When *ars3003* is deleted, the *ars3002*-associated origin, which was already the most efficient, becomes even stronger (Figure 8A, panel a). When both *ars3002* and *ars3003* are deleted, the *ars3004*-associated origin is strengthened (Figures 6C and 8B).

This inter-origin interference in a natural cluster of origins appears similar to the interference detected by Brewer and Fangman (1993) between ARS elements which were experimentally brought into close proximity in *S.cerevisiae*. However, the extent of inter-origin interference appears to be somewhat less in the *ura4* origin region than in the region of *S.cerevisiae* studied by Brewer and Fangman (1993). In both organisms, interference is manifested by suppression by one origin of initiations from nearby origins. When nearby origins in the same DNA molecule function simultaneously, the replication forks converging between them produce a triangular termination pattern in neutral/neutral 2D gel electrophoresis (Figure 3D; Brewer and Fangman, 1993). Such patterns are barely visible between closely spaced origins in *S.cerevisiae* (Brewer and Fangman, 1993), but are easily detected among the closely spaced origins of the *ura4* origin region (Figure 4, panels b–f and m). Despite the existence of readily detectable termination signals, the data suggest that in most cases just one of the three *ura4* origins fires. If all three *ura4* origins were to fire in every S phase, (i) strong bubble arcs would be associated with each of them, (ii) strong termination signals would be detected between them, and (iii) complete Y arcs would not be detectable in fragments centered on them. None of these predictions is fulfilled. Instead, the weakness of bubble signals from fragments centered over *ars3003* and *ars3004* and the fact that complete Y arc signals are considerably more prominent than termination signals from all fragments in the region suggest that, most of the time, only a single initiation occurs in the *ura4* origin region.

Interference between closely spaced origins could possibly be explained by the mechanism which prevents eukaryotic DNA from being replicated more than once per S phase. This mechanism would prevent initiation at any ARS element which had failed to fire before being passively replicated by a nearby origin. If so, then, in any cluster of origins, the origin which fires earliest in S phase would be the most active origin of the cluster.

Relationship of the ura4 origin region to replication origins in animal cells

The properties of the origins used for gene amplification in insects suggest that they are compound origins, like the *ura4* origin region. Amplification is controlled by multiple separable *cis*-acting sequence elements located between and flanking the chorion genes on the third chromosome of *Drosophila melanogaster* (reviewed in Orr-Weaver, 1991). 2D gel analyses suggest the presence of an initiation zone covering the gene region. Within this zone, a much smaller region, corresponding to one of the *cis*-acting elements, is used predominantly (Delidakis and Kafatos, 1989; Heck and Spradling, 1990). Other initiation sites may correspond to others of the *cis*-acting elements (Heck and Spradling, 1990). The initiation zone associated with an amplification origin in *Sciara coprophila* also consists of a primary initiation site flanked by weaker initiation sites (Liang *et al.*, 1993).

The data obtained with yeasts (Brewer and Fangman, 1993; this paper) and insects (Delidakis and Kafatos, 1989; Heck and Spradling, 1990; Liang *et al.*, 1993) demonstrate that the 2D gel electrophoretic properties of the large initiation zones of mammalian cells (Vaughn *et al.*, 1990; Dijkwel and Hamlin, 1992; Little *et al.*, 1993) could be due to these initiation zones being composed of multiple origins. Determination of whether or not mammalian origins are compound will require further experiments. In particular, it is essential to characterize the replicators responsible for mammalian origins. Are broad mammalian initiation zones determined by a single non-divisible replicator, or can the replicators which have been identified (Handeli *et al.*, 1989; Kitsberg *et al.*, 1993), and other replicators yet to be discovered, be subdivided into multiple elements, each capable of providing (perhaps limited) origin function?

Materials and methods

Strains and media

Escherichia coli DH5α cells (Life Technologies) were transformed with progressive deletion plasmids as described below and grown in LB medium containing ampicillin. The *S.pombe* strain *ura4*-D18, usually referred to as D18 in this paper (*ura4*-D18 *leu1*-32 *end1* h^-; Grimm *et al.*, 1988), a gift from Susan Gasser, was used as the recipient strain for transformation assays and as the parental strain for genomic alterations. For transformation purposes, cells were grown in MB (Moreno *et al.*, 1991) supplemented with 150 mg/l each of uracil and leucine. For all other purposes, cells were grown in YE (Moreno *et al.*, 1991) with (for D18 cells) or without (for all other new constructs) uracil.

Generation of progressive deletions

Plasmids pRS306-ori and pRS306-1.2 were constructed by ligating the 2.7 kbp *Bam*HI−*Eco*RI and 1.25 kbp *Eco*RI−*Bam*HI fragments (region in brace in Figure 1) between the *Bam*HI and *Eco*RI sites in the multiple cloning site of the vector pRS306 (Sikorski and Hieter, 1989), which contains the *URA3* gene, permitting selection in the D18 strain. Unidirectional sequential deletions from both ends of each insert using exonuclease III were generated as described (Henikoff, 1984) with modifications suggested by Stratagene (protocol for the pBluescriptII exonuclease III/mung bean DNA sequencing system, Stratagene). For deletions starting at the *Bam*HI site, CsCl-purified pRS306-ori or pRS306-1.2 was digested with *Bam*HI to generate recessed 3′ ends susceptible to exonuclease III attack, and also with *Sac*I to generate exonuclease III-resistant protruding 3′ ends between the *Bam*HI site and the sequencing primer (T7 primer). For deletions starting at the *Eco*RI site, the same plasmids were cut with *Eco*RI and *Kpn*I (pRS306-ori) or with *Hin*dIII and *Kpn*I (pRS306-1.2) to generate recessed and protruding 3′ ends, respectively. Subsequent incubation with exonuclease III for increasing times resulted in progressive resection of the insert while leaving the *Sac*I or *Kpn*I end intact. Mung bean nuclease was then used to generate flush ends, the plasmids were re-circularized by blunt end ligation, and then used to transform DH5α cells. Minipreps of individual plasmid clones from each time point were used to select clones with deletions of increasing size in increments of 150–250 bp.

ARS assays

The *S.pombe* strain *ura4-D18* was transformed by either of two procedures. In early experiments, we used the lithium acetate procedure according to Moreno *et al.* (1991). In later experiments, we used the lithium acetate procedure according to Gietz *et al.* (1992), except that cells were grown in MB medium. This latter procedure consumes less time and provides somewhat higher transformation frequencies than the former procedure. Successfully transformed cells were selected on MMA plates supplemented with leucine but lacking uracil (Moreno *et al.*, 1991), and the numbers of colonies were counted after incubation at 30°C for 4–5 days. We observed that colony size varied with transformation frequency: colonies transformed with plasmids capable of high transformation frequency were usually larger than colonies transformed with plasmids capable of lower transformation frequencies, presumably reflecting differences in plasmid replication efficiency. In some cases, extremely small colonies were detected. These were ignored during counting, because they could not grow in liquid medium.

Construction of new strains

Three new strains were made using standard cloning and one step gene disruption (Rothstein, 1983) techniques. The *ura4 Hin*dIII fragment was blunt-ended with Klenow polymerase and cloned into the *Eco*RV site of the plasmid pBluescript KS^+ (Stratagene) in which the *Hin*dIII site had been destroyed (pΔHIII*ura4*). To replace *ars3002* with the *ura4* gene, p4.1 (the 4.1 kbp *Bam*HI−*Hin*dIII fragment which contains *ars3002*, cloned in pBluescript KS^+) was first linearized with *Eco*RV and then partially digested with *Nsi*I. The digestion products were ligated with the 1.8 kbp *Hin*cII−*Pst*I *ura4* fragment derived from pΔHIII*ura4*. Of the resulting plasmids, one containing the desired deletion of *ars3002* (pΔ3002::*ura4*) was selected, confirmed to lack ARS activity, and then linearized with *Bam*HI and *Hin*dIII, and the resulting 5.1 kbp fragment was used for transforming D18 cells (Figure 4). To replace *ars3003* with the *ura4* gene, the 5.6 kbp *Hin*dIII−*Eco*RV fragment containing *ars3003* was cloned into the *Hin*dIII and *Eco*RV sites of pBluescript KS^+. The resulting plasmid (p5.6) was digested with *Bst*BI and *Avr*II to remove *ars3003*, gel purified, and then ligated with the *Cla*I−*Xba*I *ura4* fragment derived from pΔHIII*ura4*. The resulting plasmid (pΔ3003::ura4) was confirmed to lack ARS activity. Its *Bgl*II−*Hin*dIII fragment was used for transformation of D18 h^- cells (Figure 8A). For removal of both *ars3002* and *ars3003*, first *ars3003* was removed from p5.6 by digesting it with *Bst*BI and *Avr*II, end filling with Klenow polymerase, gel purification and self-ligation, resulting in pΔ3003. The 3.9 kbp *Xba*I−*Bgl*II fragment from pΔ3003 was then cloned into the *Xba*I/*Bgl*II sites of pΔ3002::*ura4*. The resulting plasmid (pΔ3003, Δ3002::*ura4*) lacked ARS activity. Its *Xba*I−*Hin*dIII fragment was used to transform D18 cells, thus creating Δ3002, Δ3003 cells (Figures 6C and 8B).

Transformations for the purpose of new strain construction were done as described above for ARS assays. Cells from selected colonies were grown for several generations in non-selective medium to permit loss of plasmids or recircularized transforming DNA containing the *ura4* gene and then replated on selective plates. DNA was extracted from the resulting colonies and analyzed by restriction digestion and Southern blotting to ensure that the desired transformant had been obtained.

DNA isolation

DNA was isolated from logarithmically growing cells ($1.2–1.8 \times 10^7$ cells/ml) using the glass bead method as described earlier (Huberman *et al.*, 1987) except that for all neutral/neutral 2D electrophoreses and the neutral/alkaline 2D electrophoreses of DNA from the D18 strain, we took advantage of the observation (J.A.Sanchez, unpublished data) that the use of sodium azide just before harvesting *S.pombe* cells helps to preserve replication intermediates, hence increasing sensitivity, especially for neutral/neutral gels. When used, sodium azide was added to the cells just before harvesting, to a final concentration of 0.1%. The cells were simultaneously cooled on ice and processed for DNA isolation. All other steps were essentially the same as previously described (Huberman *et al.*, 1987; Zhu *et al.*, 1992a).

2D gel electrophoreses

Approximately 140 μg of DNA for each neutral/neutral gel or 400–500 μg DNA for each neutral/alkaline gel were digested to completion with a 5-fold excess of the appropriate enzyme(s) in total volumes of 3–6 ml. The DNA was ethanol-precipitated and resuspended in smaller volumes (0.5–1 ml) of TE. For the enrichment of replicating DNA, BND-cellulose fractionation was performed as described (Huberman *et al.*, 1987). In each case all the caffeine wash DNA was loaded onto a 0.4% agarose gel, and first dimension electrophoresis was performed as described (Huberman *et al.*, 1987). For the second dimension of neutral/neutral electrophoresis, the conditions of Brewer and Fangman (1987) were employed, with the modification that for fragments larger than 6 kbp the second dimension was in a 0.6% gel at 2 V/cm for 14–16 h. The second dimension of neutral/alkaline gels was done as described (Huberman *et al.*, 1987; Nawotka and Huberman, 1988).

Southern blotting and hybridization

DNA was transferred to GeneScreen (Dupont) membranes following 10–15 min depurination in 0.25 M HCl, using 0.4 M NaOH and 1 M NaCl as transfer buffer. The DNA was crosslinked to the membrane using a Stratalinker (Stratagene; program autocrosslink 1200), and before hybridization the membranes were incubated once for 30 min in boiling 0.1× SSC, 0.1% SDS. Prehybridization (3–7 h) and hybridization (15–22 h) with heat-denatured ^{32}P-labeled probes were done at 65°C in 6× SSPE, 5× Denhardt's solution, 0.5% SDS and 150 μg/ml denatured salmon sperm DNA. Dextran sulfate (10%) was included in the hybridization buffer. Probes were synthesized by random primer labeling using gel- and GeneClean (Bio101)-purified DNAs. The membranes were washed at room temperature with solutions pre-heated to 65°C: twice with 1 mM EDTA, 40 mM sodium phosphate, pH 7.4, containing 5% SDS, and four times with the same buffer containing 1% SDS. The membranes were then exposed to phosphor storage screens and, after 1–5 days, scanned with a PhosphorImager (Molecular Dynamics).

Image processing

The 16-bit TIFF files from the PhosphorImager were transferred to a Macintosh computer and opened by IPLab Spectrum (Signal Analytics Corporation). They were then linearly scaled between the lowest signal value and an appropriate higher value to provide the desired signal intensities (this operation is analogous to varying the exposure time during conventional autoradiography). The scaled pictures were converted to 8-bit TIFF format, then converted to EPS format and placed into a Macintosh drawing program for figure preparation. Final images were printed with a dye sublimation printer.

Acknowledgements

We are grateful to Mitsuhiro Yanagida and Hisanori Kurooka, who provided us with cosmid clones of *S.pombe* DNA covering the region of interest, and to Susan Gasser, who sent us the *ura4-D18* strain of *S.pombe*. Nicole Symons and Tatyana Danilenko performed some of the transformation frequency assays. Christine Brun, Bill Burhans, Soo-mi Kim, David Kowalski, Martin Weinberger, John Yates and Yeup Yoon provided constructive criticism of the manuscript. D.D. is thankful to Kutir Mahavidyalaya Chakkey, Jaunpur, India, for granting him an academic leave. This research was supported by grants from the National Institutes of Health (PO1-GM44119 and RO1-GM49294).

References

Brewer,B.J. and Fangman,W.L. (1987) *Cell*, **51**, 463–471.
Brewer,B.J. and Fangman,W.L. (1993) *Science*, **262**, 1728–1731.
Burhans,W.C. and Huberman,J.A. (1994) *Science*, **263**, 639–640.
Caddle,M.S. and Calos,M.P. (1994) *Mol. Cell. Biol.*, **14**, 1796–1805.
Campbell,J.L. and Newlon,C.S. (1991) In Broach,J.R., Pringle,J.R. and Jones,E.W. (eds), *The Molecular Biology and Cellular Biology of the Yeast Saccharomyces: Genome Dynamics, Protein Synthesis, and Energetics*. Cold Spring Harbor Laboratory Press, Cold Spring Harbor, NY, Vol. 1, pp. 41–146.
Delidakis,C. and Kafatos,F.C. (1989) *EMBO J.*, **8**, 891–901.
Deshpande,A.M. and Newlon,C.S. (1992) *Mol. Cell. Biol.*, **12**, 4305–4313.
Dijkwel,P.A. and Hamlin,J.L. (1992) *Mol. Cell. Biol.*, **12**, 3715–3722.
Gietz,D., St John,A., Woods,R.A. and Schiestl,R.H. (1992) *Nucleic Acids Res.*, **20**, 1425.
Grimm,C., Kohli,J., Murray,J. and Maundrell,K. (1988) *Mol. Gen. Genet.*, **215**, 81–86.
Handeli,S., Klar,A., Meuth,M. and Cedar,H. (1989) *Cell*, **57**, 909–920.
Heck,M.M.S. and Spradling,A.C. (1990) *J. Cell Biol.*, **110**, 903–914.
Henikoff,S. (1984) *Gene*, **28**, 351–359.
Hsiao,C.-L. and Carbon,J. (1979) *Proc. Natl Acad. Sci. USA*, **76**, 3829–3833.
Huang,R.-Y. and Kowalski,D. (1993) *EMBO J.*, **12**, 4521–4531.
Huberman,J.A., Spotila,L.D., Nawotka,K.A., El-Assouli,S.M. and Davis,L.R. (1987) *Cell*, **51**, 473–481.
Kitsberg,D., Selig,S., Keshet,I. and Cedar,H. (1993) *Nature*, **366**, 588–590.
Liang,C., Spitzer,J.D., Smith,H.S. and Gerbi,S.A. (1993) *Genes Dev.*, **7**, 1072–1084.
Linskens,M.H.K. and Huberman,J.A. (1988) *Mol. Cell. Biol.*, **8**, 4927–4935.
Linskens,M.H.K. and Huberman,J.A. (1990) *Nucleic Acids Res.*, **18**, 647–652.
Little,R.D., Platt,T.H.K. and Schildkraut,C.L. (1993) *Mol. Cell. Biol.*, **13**, 6600–6613.
Maundrell,K., Hutchison,A. and Shall,S. (1988) *EMBO J.*, **7**, 2203–2209.
Moreno,S., Klar,A. and Nurse,P. (1991) *Methods Enzymol.*, **194**, 795–823.
Nawotka,K.A. and Huberman,J.A. (1988) *Mol. Cell. Biol.*, **8**, 1408–1413.
Orr-Weaver,T.L. (1991) *BioEssays*, **13**, 97–105.
Rivier,D.H. and Rine,J. (1992) *Science*, **256**, 659–663.
Rothstein,R.J. (1983) *Methods Enzymol.*, **101**, 202–211.
Sikorski,R.S. and Hieter,P. (1989) *Genetics*, **122**, 19–27.
Struhl,K., Stinchcomb,D.T., Scherer,S. and Davis,R.W. (1979) *Proc. Natl Acad. Sci. USA*, **76**, 1035–1039.
Toda,T., Nakaseko,Y., Niwa,O. and Yanagida,M. (1984) *Curr. Genet.*, **8**, 93–97.
Vaughn,J.P., Dijkwel,P.A. and Hamlin,J.L. (1990) *Cell*, **61**, 1075–1087.
Zhu,J., Brun,C., Kurooka,H., Yanagida,M. and Huberman,J.A. (1992a) *Chromosoma*, **102**, S7–S16.
Zhu,J., Newlon,C.S. and Huberman,J.A. (1992b) *Mol. Cell. Biol.*, **12**, 4733–4741.

Received on March 25, 1994; revised on May 16, 1994